J Mater Sci (2008) 43:402–405
DOI 10.1007/s10853-007-2203-8

LETTER

Subcritical crack growth in SiAlON ceramics from a modified static lifetime test including multiple use of survivals

M. Riva · M. J. Hoffmann · R. Oberacker · T. Fett

Received: 16 August 2007 / Accepted: 28 September 2007 / Published online: 16 October 2007

SiAlON ceramics are important materials for applications under high mechanical and thermal stress such as cutting tools or engine components. These solid solutions offer a wide variety of microstructures and properties depending on composition and sintering parameters. As observed in most ceramics, also for SiAlON, the effect of subcritical crack growth has to be expected. However, preliminary tests on this material have shown very little subcritical crack growth, whereby the determination of the crack growth exponent n causes difficulties. This work przesents a new method to obtain statistically more significant results.

SiAlON ceramics can be derived from both α- and β-silicon nitride modifications by substituting silicon by aluminium and nitrogen by oxygen. The possibility to stabilize two crystal structures offers the opportunity to design materials ranging from pure α-, mixed α/β-, up to pure β-SiAlONs. In general, α-SiAlONs are in the form of equiaxed grains with high hardness and good wear resistance, but low fracture toughness, whereas β-SiAlONs have elongated grains with high fracture toughness, but relatively low hardness. To combine the advantages of both SiAlONs, α/β-SiAlON composites have been developed over the past years by different mechanisms including the choice of starting powders, sintering parameters and the amount of additives. Sintering additives are necessary because SiAlONs are densified by a liquid phase sintering process like silicon nitride materials [1].

M. Riva (✉) · M. J. Hoffmann · R. Oberacker · T. Fett
Institut für Keramik im Maschinenbau, Universität Karlsruhe, Karlsruhe, Germany
e-mail: marco.riva@ikm.uka.de

T. Fett
Forschungszentrum Karlsruhe, Institut für Materialforschung II, Karlsruhe, Germany

In the present work, Nd_2O_3 was used as sintering additive in the starting powder mixtures for the fabrication of a mixed α/β-SiAlON [2]. The starting powders Si_3N_4 (UBE, SN-E10), AlN (H. C. Starck, grade C), Al_2O_3 (Alcoa, CTC 20), Nd_2O_3 (Alfa Aesar, Neodymium (III) Oxide REacton) were attrition-milled for 4 h with silicon nitride milling balls in isopropanol. The slurry was subsequently dried in a rotatory evaporator, and finally sieved. Consolidation of the powder mixture into rectangular plates has been obtained by uniaxial pressing in a steel matrix and subsequent cold isostatic pressing at 400 MPa pressure. Sintering was performed in nitrogen atmosphere in a BN-crucible using a hotisostatic press with a graphite resistance heater. The powder compacts were heated at a rate of 10 K/min to the maximum sintering temperature of 1,830°C. During this heat-up phase, the pressure was kept below 1 MPa. When having reached the maximum temperature, the pressure was held at 1 MPa for 15 min, and then increased to 10 MPa for another 45 min.

The composition investigated was calculated according to the general SiAlON formula [3]

$$M_xSi_{12-(m_{SiAlON}+n_{SiAlON})}Al_{m_{SiAlON}+n_{SiAlON}}O_{n_{SiAlON}}N_{16-n_{SiAlON}}$$

with the coefficients $m_{SiAlON} = 0.5$ and $n_{SiAlON} = 1.0$, and lays near the Si_3N_4 corner of the SiAlON plane (Fig. 1a). The amount of oxygen in silicon nitride and aluminium nitride powders has been taken into consideration for the calculation of the starting powder mixture. To improve densification behaviour, the powder contains 10% excess of the sintering additive Nd_2O_3.

The so obtained plates exhibit a relative density of 99.4–99.8% of the theoretical density. The SEM micrograph (Fig. 1b) shows a balanced microstructure with a bright phase with an equiaxed grain morphology that corresponds

to α-SiAlON and dark grains with elongated morphology corresponding to β-SiAlON. The small bright spots are rich in Neodymium and represent the small fraction of amorphous grain boundary phase located at triple junctions. No other crystalline phase could be detected by XRD after sintering. X-ray diffraction analysis of the samples showed an α/β-ratio of 55/45.

Specimens for the four-point-bending tests were machined from dense plates according to the European Standard EN 843-1: 1995 and have the final dimensions of 3 mm × 4 mm × 48 mm.

In order to determine failure behaviour, first a number of $N = 27$ inert strength tests were performed in air at a loading rate of about 250 MPa/s. The strength distribution is shown in Fig. 2a in Weibull representation resulting in the Weibull parameters of

$$m = 6.2\ [4.6;\ 7.7],\ m_{\mathrm{corr}} = \ 5.9,\ \sigma_0 = 904\,\mathrm{MPa}[854; 958]$$

These values were obtained by applying the maximum-likelihood procedure [4]. The numbers in brackets are the 90% confidence intervals according to [5], and m_{corr} is the unbiased Weibull exponent suggested by Thoman et al. [4].

Subcritical crack growth is governed by the stress intensity factor K, and for a given material, there is a unique relation between the crack growth rate V and K_{I}, which very often can be described by a power–law relation

$$V = A^* \left(\frac{K_{\mathrm{I}}}{K_{\mathrm{Ic}}} \right)^n \tag{1}$$

with the parameters A^* and n depending on the material, the temperature and the environment. The parameters of relation (1) are very often determined in static lifetime tests.

To determine these parameters, $N = 27$ lifetime tests were performed at $\sigma = \sigma_1 = 700$ MPa. During load application, eight specimens failed spontaneously, four after regular lifetimes $t_f < t_0 = 280$ h, and 15 specimens survived (circles in Fig. 2b). Evaluation of these lifetime

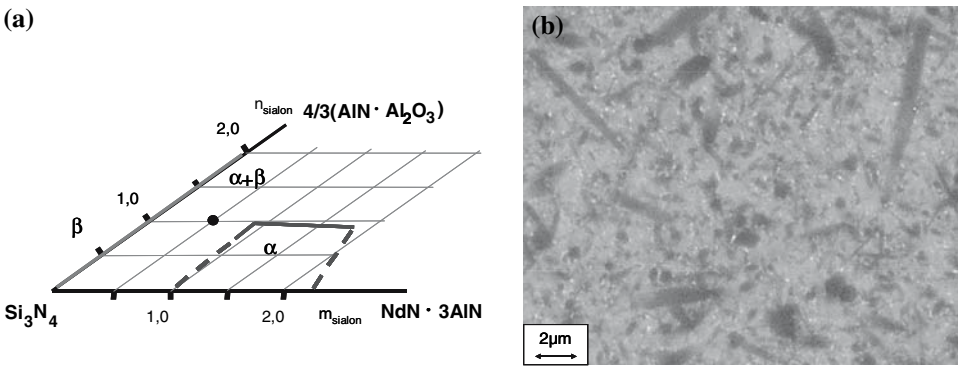

Fig. 1 (**a**) Investigated composition in the system Nd–Si–Al–O–N [2]. (**b**) SEM-micrograph of the α/β-SiAlON with $m_{\mathrm{SiAlON}} = 0.5$, $n_{\mathrm{SiAlON}} = 1.0$ and 10% of Nd_2O_3 excess

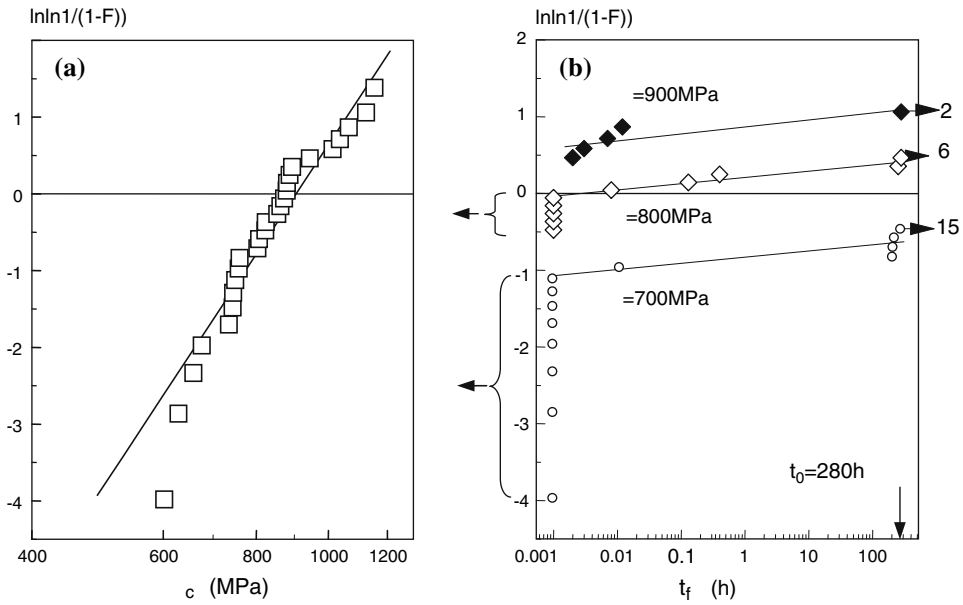

Fig. 2 (**a**) Weibull representation of the inert strength, (**b**) lifetimes (solid symbols: regular failure, symbols with arrows: fracture during loading or survivals)

results by application of the truncated maximum-likelihood procedure by Lawless (see e.g. [6]) yields

$$m = 0.04552,\ t_0 = 5.5 \times 10^{-7} \text{ resulting in } n = 138$$

Especially for materials with such a large crack growth exponent, the number of spontaneous failures during load application and survivals is larger than the number of tests with regular failure. A special modification of lifetime tests is therefore proposed.

In order to get additional information on the subcritical crack growth behaviour, the authors recommend performing further lifetime tests with the survivals on an increased load level. The necessary procedure will be outlined below. First, the procedure will be explained for the simple case of the power–law crack growth relation according to (1). Then, it will be applied to static lifetime measurements on SiAlON in distilled water of 20°C.

Using the definition of the stress intensity factor and the power–law relation of subcritical crack growth, integration of (1) yields for arbitrary time-dependent stresses $\sigma(t)$

$$\int_0^{t_f} \sigma(t)^n \, dt = B\sigma_c^{n-2}[1 - (\sigma_f/\sigma_c)]^{n-2} \tag{2}$$

as outlined in detail in [6]. The material parameter B comprises the inert strength σ_c and the fracture toughness K_{Ic}

$$B = \frac{2K_{Ic}^2}{A^* Y^2 (n-2)}. \tag{3}$$

(with $Y = 1.3$ for semi-circular surface cracks).

Let us now consider a lifetime test first carried out at load $\sigma = \sigma_1$. Some of the specimens may fail already during the loading step. Other specimens will fail before $t = t_0$ is reached, resulting in regular lifetimes t_f. Finally, after the time t_0, a few survivals will be found. For these specimens, the applied load is increased to $\sigma_2 > \sigma_1$ and the lifetime of the survivals on preceding load σ_1 is determined. During load increase also some of the specimens may fail immediately. We identify this extended test now as a lifetime test under step-shaped loading (Fig. 3). The load on the first level is σ_1, and the time $t = t_0$ is the time limit defining the survivals of the first test.

The load history for this test (Fig. 3) is

$$\sigma(t) = \begin{cases} \sigma_1 & \text{for } t \le t_0 \\ \sigma_2 & \text{for } t > t_0 \end{cases} \tag{4}$$

Inserting (4) in (2) yields

$$\sigma_1^n t_f = B\sigma_c^{n-2}[1 - (\sigma_1/\sigma_c)]^{n-2} \quad \text{for } t_f \le t_0 \tag{5}$$

and

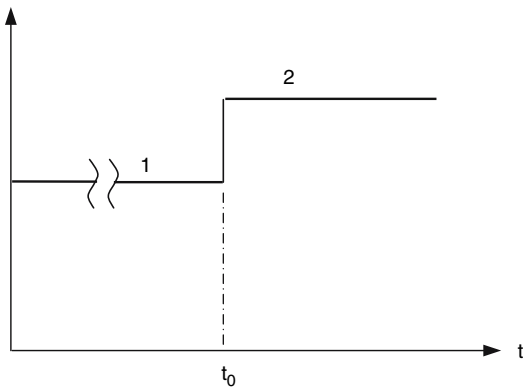

Fig. 3 Load–time history for a lifetime test under step-shaped load

$$\sigma_1^n t_0 + \sigma_2^n (t_f - t_0) = B\sigma_c^{n-2}[1 - (\sigma_2/\sigma_c)]^{n-2} \quad \text{for } t_f > t_0 \tag{6}$$

From the system (5) and (6), the two parameters n and A^* can be determined, for instance, using least-squares procedure. It is assumed that a number of N samples are tested at high loading rates in an inert environment to give the strength distribution with the individual values $\sigma_{c,i}$. In a second series, also involving N specimens, the individual lifetimes $t_{f,i}$ are measured.

For an arbitrarily chosen set of parameters (A^*, n), a series of lifetimes can be computed for the N tested samples. From (5) and (6), these lifetimes result as

$$t_{f,1,i} = B\sigma_{c,i}^{n-2}\sigma_1^{-n}[1 - (\sigma_1/\sigma_{c,i})]^{n-2} \quad \text{for } \sigma_f = \sigma_1 \tag{7}$$

$$t_{f,2,i} = B\sigma_{c,i}^{n-2}\sigma_2^{-n}[1 - (\sigma_2/\sigma_{c,i})]^{n-2} - \left(\frac{\sigma_1}{\sigma_2}\right)^n t_0 \quad \text{for } \sigma_f = \sigma_2 \tag{8}$$

where $t_{f,2,i}$ in (8) is the time cumulated on the upper load level exclusively, i.e. $t_{f,2} = t_f - t_0$. The individual computed and measured lifetimes are then fitted by minimizing the deviations between the two quantities. This can, for instance, be done by minimizing

$$\sum_{i=1}^{N} \left(\log \frac{t_{f,\text{computed},i}}{t_{f,\text{measured},i}}\right)^2 = \min \tag{9}$$

This numerical treatment requires special care in programming, since negative values of $t_{f,\text{computed},i}$ have to be avoided.

In order to vary the parameters n and A^* systematically, a FORTRAN program is used, based on the Harwell computer subroutine VA02AD.

If a sufficiently large number of survivals are available after the tests on stress level σ_2, the procedure can be

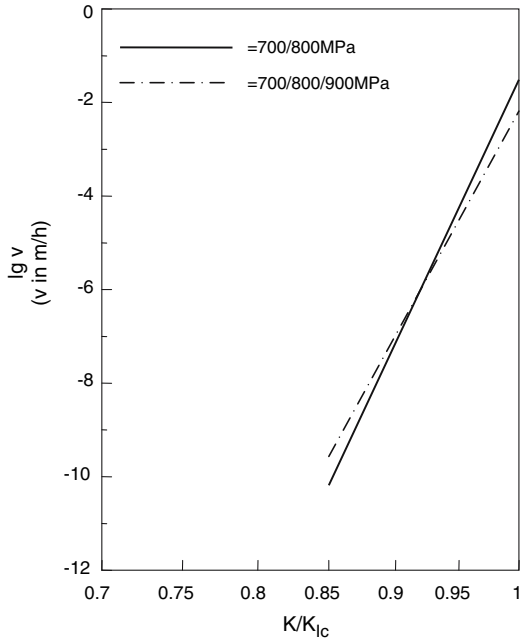

Fig. 4 Comparison of the power–law solutions obtained from the evaluation of the two lower stress levels (solid line) and the evaluation of all data (dash–dotted line)

repeated on an increased stress level $\sigma_3 > \sigma_2$. Then, it results from (2) that

$$t_{f,3,i} = \sigma_{c,i}^{n-2}\sigma_3^{-n}[1-(\sigma_3/\sigma_{c,i})]^{n-2} - \left(\frac{\sigma_1}{\sigma_3}\right)^n t_0 - \left(\frac{\sigma_2}{\sigma_3}\right)^n t_0 \tag{10}$$

with the time $t_{f,3}$ cumulated on the load level σ_3 exclusively.

After the tests performed at $\sigma = \sigma_1 = 700$ Mpa, the load for the survived specimens was increased up to $\sigma_2 = 800$ MPa. Before this stress level was reached, a number of five specimens failed spontaneously. Out of the remaining samples, four specimens failed during the next 280 h (squares in Fig. 2b). Six specimens survived this second time span. The load was increased once more and the survivals were tested now at $\sigma_3 = 900$ MPa. Two specimens survived on this load level.

First, only the two lower load levels were evaluated. Application of Eqs. (7–9) resulted in

$$n = 122.8,\ A^* = 3.05 \times 10^{-2}\ \text{m/h} \tag{11}$$

In a second evaluation of all three load levels with an increased number of test results, the additional application of Eq. (10) yields

$$n = 104.6,\ A^* = 6.5 \times 10^{-3}\ \text{m/h} \tag{12}$$

The solutions obtained from the evaluation of two and three load levels are represented in Fig. 4 by the straight lines. Since the higher n-value is related to the lower A^*, the two lines represent nearly the same region of data. In this context, it should be mentioned that different solutions should always be assessed by the pair of parameters and not by the individual n or A^*-values.

Conclusions

The large crack growth exponent n of more than 100 obtained for a SiAlON ceramic investigated under distilled water indicates hardly any environmental-assisted subcritical crack growth. Compared to silicon nitride ceramics with a characteristic crack growth exponent n of about 40 [7], this behaviour can be referred to a smaller volume fraction of amorphous grain boundary phase present in the tested SiAlON-ceramic, like shown in the SEM-micrograph (Fig. 1b). Therefore, the material presented here has much higher potential for applications under moisture and water. The large number of spontaneous failure and survivals makes the development of a modified procedure necessary, in order to obtain a significant database.

Acknowledgement The authors would like to thank the Deutsche Forschungsgemeinschaft DFG for financing this work within the SFB 483.

References

1. Shen ZJ, Ekström T, Nygren M (1996) J Am Ceram Soc 79:721
2. Holzer S, Geßwein H, Hoffmann MJ (2003) Key Eng Mat 237:43
3. Ekström T, Nygren M (1992) J Am Ceram Soc 75:259
4. Thoman DR, Bain LJ, Antle CE (1969) Technometrics 11:445
5. European Standard ENV 843–5, Advanced monolithic ceramics—mechanical tests at room temperature—statistical analysis
6. Munz D, Fett T (1999) CERAMICS, failure, material selection, design. Springer-Verlag, Heidelberg, Germany
7. Lube T, Dusza J (2007) J Eur Ceram Soc 27:1203